



Published in final edited form as:

Neurobiol Dis. 2015 January ; 73: 348–355. doi:10.1016/j.nbd.2014.10.015.

BTBR *ob/ob* mice as a novel diabetic neuropathy model: neurological characterization and gene expression analyses

Phillipe D. O'Brien¹, Junguk Hur¹, John M. Hayes¹, Carey Backus¹, Stacey A. Sakowski², and Eva L. Feldman^{1,2,*}

¹Department of Neurology, University of Michigan, Ann Arbor, MI 48109, USA

²A. Alfred Taubman Medical Research Institute, University of Michigan, Ann Arbor, MI 48109

Abstract

Given the lack of treatments for diabetic neuropathy (DN), a common diabetic complication, accurate disease models are necessary. Characterization of the leptin-deficient BTBR *ob/ob* mouse, a type 2 diabetes model, demonstrated that the mice develop robust diabetes coincident with severe neuropathic features, including nerve conduction deficits and intraepidermal nerve fiber loss by 9 and 13 weeks of age, respectively, supporting its use as a DN model. To gain insight into DN mechanisms, we performed microarray analysis on sciatic nerve from BTBR *ob/ob* mice, identifying 1,503 and 642 differentially expressed genes associated with diabetes at 5 and 13 weeks, respectively. Further analyses identified overrepresentation of inflammation and immune-related functions in BTBR *ob/ob* mice, which interestingly were more highly represented at 5 weeks, an observation that may suggest a contributory role in DN onset. To complement the gene expression analysis, we demonstrated that protein levels of select cytokines were significantly upregulated at 13 weeks in BTBR *ob/ob* mouse sciatic nerve. Furthermore, we compared our array data to that from an established DN model, the C57BKS *db/db* mouse, which reflected a common dysregulation of inflammatory and immune-related pathways. Together, our data demonstrate that BTBR *ob/ob* mice develop rapid and robust DN associated with dysregulated inflammation and immune-related processes.

Type 2 diabetes (T2D) has reached epidemic proportions worldwide, affecting over 382 million individuals (1). The associated hyperglycemia, insulin resistance, and/or obesity leads to microvascular complications that impact multiple organs and tissues, including the eyes, kidney, and peripheral nerves. Peripheral diabetic neuropathy (DN), the most common microvascular complication (2), is characterized by distal-to-proximal nerve damage that

*Corresponding author: Eva L. Feldman, MD, PhD, Russell N. DeJong Professor of Neurology, 5017 AAT-BSRB, 109 Zina Pitcher Place, Ann Arbor, Michigan 48109, United States, Phone: 001734 763-7274 / Fax: 001 734 763-7275, efeldman@umich.edu.

P.D.O.B. conducted animal experiments, performed RT-qPCR validation and immunoassays, researched data, and wrote the manuscript. J.H. researched data and reviewed and edited the manuscript. J.M.H. and C.B. conducted animal experiments. S.A.S. contributed to discussion and reviewed and edited the manuscript. E.L.F. designed and directed the study, contributed to discussion, and reviewed the manuscript.

No potential conflicts of interest relevant to this article were reported.

Publisher's Disclaimer: This is a PDF file of an unedited manuscript that has been accepted for publication. As a service to our customers we are providing this early version of the manuscript. The manuscript will undergo copyediting, typesetting, and review of the resulting proof before it is published in its final citable form. Please note that during the production process errors may be discovered which could affect the content, and all legal disclaimers that apply to the journal pertain.

promotes pain and loss of sensation. Sensory deficits combined with poor wound healing can trigger foot ulcer development and non-traumatic lower limb amputations, contributing to the severe morbidity of DN (3).

Although the exact etiology remains unclear, the consensus is that DN results from metabolic and physiological imbalances within the peripheral nerve. Persistent hyperglycemia-induced oxidative stress promotes nerve damage (4,5), and evidence also suggests dyslipidemia contributes to aberrant nerve function (6,7). Numerous biochemical processes, including the formation of advanced glycation end products, increased NADPH oxidase activity, activation of poly ADP ribose polymerase, and inflammation, are implicated in DN (4,8,9). Thus, elucidating the precise mechanisms underlying nerve injury is of paramount importance to develop successful therapies.

Various mouse models exist that mimic a diabetes-like phenotype and exhibit key DN features (10); however, additional models that accurately recapitulate the complex pathogenesis of T2D are required to gain insight into DN etiology and support translational studies. The leptin-deficient BTBR *ob/ob* mouse is a robust model of T2D (11,12); they are hyperphagic and present with early obesity, insulin resistance, and hyperglycemia at a severity greater than that observed in C57BL6 *ob/ob* mice (11,13,14). Additionally, these mice develop renal complications closely mimicking human diabetic nephropathy, evidenced by glomerular hypertrophy, capillary basement membrane thickening, and loss of podocytes (13). The effects on the peripheral nerve in this model, however, have not been characterized.

In the current study, the primary objective was to characterize the neurological phenotype in BTBR *ob/ob* mice. We confirm that BTBR *ob/ob* mice present with robust features of T2D and exhibit an early and severe neuropathy. We further identified altered genes and pathways in sciatic nerve (SCN) using arrays and bioinformatics analyses, demonstrating that inflammation and immune response factors are overrepresented early in the disease course. These pathways are also altered in SCN of an established DN model, the C57BKS *db/db* mouse, further supporting the BTBR *ob/ob* data. Together, our findings suggest that dysregulation of the immune response may play a critical role in DN pathogenesis and support our contention that BTBR *ob/ob* mice are a valid DN model for mechanistic and therapeutic development research.

RESEARCH DESIGN AND METHODS

Animals

Male BTBR *ob/+* and *ob/ob* mice (BTBR.Cg-*Lep^{ob}*/WiscJ, Jackson Laboratory, Bar Harbor, ME) were fed a standard diet (5LOD; 13.4% kcal fat; Research Diets, NJ). All procedures were in compliance with protocols established by the Diabetic Complications Consortium (DCC) (15) and approved by the University of Michigan (U-M) University Committee on Use and Care of Animals (UCUCA). Daily monitoring and maintenance of mice was provided by the U-M Unit for Laboratory Animal Medicine (ULAM).

Metabolic and Neuropathic Phenotyping

Phenotyping of BTBR *ob/+* and *ob/ob* mice included metabolic and neurological measures to document diabetes onset, duration, and related neurological changes. Body weights and fasting blood glucose (FBG; 4 h fast) were measured weekly. Percent glycosylated hemoglobin (%GHb) was measured by the Chemistry Core at the Michigan Diabetes Research and Training Center (MDRTC). Plasma insulin measurements and fast protein liquid chromatography (FPLC) analysis for cholesterol and triglycerides were performed by the National Mouse Metabolic Phenotyping Center (MMPC; Vanderbilt, TN). Hindpaw thermal latency and nerve conduction velocities (NCVs) were measured according to published protocols (7,16). At study termination, intraepidermal nerve fiber (IENF) density profiles were determined as previously described (16).

Affymetrix Microarray Analyses

Total RNA was isolated from SCN of 5 (n=8) and 13 (n=6) week BTBR *ob/+* and *ob/ob* mice using the silica gel-based RNeasy Mini Kit (QIAGEN, Valencia, CA). RNA integrity and concentration was measured prior to hybridizing to the Affymetrix Mouse Genome 430 2.0 microarray (Santa Clara, CA) by the U-M DNA Sequencing Core as previously described (17). Microarray data files were normalized using the BrainArray Custom Chip Definition File version 16 (18) and quality was assessed using the affyAnalysisQC.R package (<http://arrayanalysis.org/>) with BioConductor (19). Intensity-based moderated T-test (IBMT) identified differentially expressed genes (DEGs) using a false discovery rate (FDR) < 0.05 cutoff. DEGs were obtained between different genotypes (*ob/+* versus *ob/ob*) for each time point or between age groups (5 weeks versus 13 weeks) for each genotype. For array data validation, DEGs were ranked by fold-change and 8-10 of the top 4% most highly altered DEGs were selected for analysis by real time RT-PCR (RT-qPCR) as previously described (17) using the endogenous reference gene YWHAZ. Primers were selected using PrimerBank (20) and purchased from Integrated DNA Technologies (Supplementary Table 1).

Microarray data were analyzed using our established in-house microarray data analysis pipeline (17,21). Over-represented biological functions among the DEGs were identified by Gene Set Enrichment Analysis (GSEA) using Database for Annotation, Visualization and Integrated Discovery (DAVID; <http://david.abcc.ncifcrf.gov/>) (22,23). Biological functions, represented by Gene Ontology (GO; <http://www.geneontology.org/>) terms and Kyoto Encyclopedia of Genes and Genomes (KEGG; <http://www.genome.jp/kegg/>) pathways, with a Benjamini-Hochberg (BH) corrected P-value < 0.05 were deemed significant. Heat-maps were generated using the top 10 most over-represented biological functions in each DEG set and clustered based on significance values (log-transformed BH-corrected P-values) to visually represent the overall similarity and differences between the DEGs. DEGs from 5- and 13-week BTBR *ob/ob* mice were also compared to a previously published data set from 24-week C57BKS *db/db* mice (17) to identify common DEGs associated with DN pathogenesis across models.

Cytokine Analyses

To investigate the role of inflammation, cytokine levels were analyzed in SCN from an additional cohort of 5- and 13-week BTBR *ob/+* and *ob/ob* mice. SCN were homogenized and protein lysates were analyzed using MILLIPLEX xMAP magnetic bead technology (Millipore, Billerica, MA) with an MMP12 (MMMP3MAG-79K) and a custom Cytokine/Chemokine panel (MCYTOMAG-70K) to assess protein levels for 16 pre-selected targets (Supplemental Table 2). Immunoassays used a Bio-Plex200 multiplex array system with Bio-Plex Manager™ 6.0 software (BioRad, Hercules, CA) according to the manufacturer's instructions.

Statistical Analysis

Statistical analyses utilized GraphPad Prism Software, Version 6 (GraphPad Software). A two-tailed T-test was performed to compare the BTBR *ob/+* mice to *ob/ob* mice. Values are reported as the mean \pm SEM.

RESULTS

Metabolic phenotyping was first performed to delineate the course of diabetes. BTBR *ob/ob* mice exhibit increased body mass compared to *ob/+* controls beginning at 5 weeks (Fig. 1A) and a 1.7-fold and 3.6-fold increase in fasting blood glucose (FBG) at 5 and 13 weeks, respectively (Fig. 1B). Similarly, percent glycosylated hemoglobin (%GHb) was 1.2-fold higher in *ob/ob* mice at 5 weeks and 2.1-fold higher at 13 weeks, reflecting progressive hyperglycemia (Fig. 1C). Plasma insulin levels were elevated in BTBR *ob/ob* mice at 5 weeks (10.7-fold) and remained elevated at 13 weeks (13.1-fold)(Fig. 1D), and FPLC lipid fraction analysis indicated that plasma cholesterol and triglyceride levels were also elevated at both time points (Figs. 1E, 1F). FPLC further revealed a sinistral shift in the HDL fraction of 5-week BTBR *ob/ob* mice, and a similar peak shift was observed along with an increase in HDL cholesterol in 13-week *ob/ob* mice, indicating increased uptake of cholesterol at both time points (Supplementary Fig. 1A, 1B). Significant increases in vLDL triglyceride levels were also present in BTBR *ob/ob* mice at 5 and 13 weeks (Supplementary Fig. 1C, 1D). Together, these data confirm that hyperglycemia and dyslipidemia are features of BTBR *ob/ob* mice.

To characterize neuropathy in BTBR *ob/ob* mice, thermal hindpaw latency was measured at 9 weeks and electrophysiological NCVs and IENF densities were measured at 9 and 13 weeks. The latency of hindpaw response to a heat stimulus was significantly increased at 9 weeks (Fig.2A). Both sciatic motor (MNCV) and sural sensory (SNCV) NCVs were significantly slower in BTBR *ob/ob* mice compared to age-matched *ob/+* controls; MNCV was reduced by 29% at 9 weeks and by 40% at 13 weeks, and SNCV was decreased by 16% at 9 weeks and 20% at 13 weeks (Fig. 2B, 2C). Protein gene product 9.5 (PGP9.5) staining of footpads revealed a 19% reduction in intra epidermal nerve fiber (IENF) density in the hind paw of BTBR *ob/ob* mice at 13 weeks compared to controls (Fig. 2D,2E). Overall, the observed increased hindpaw latency, decreased NCVs, and reduced IENF density confirm that BTBR *ob/ob* mice develop early and robust neuropathy, as evidenced by changes which

are representative of the characteristic nerve fiber damage and distal sensory defects commonly present in human subjects with diabetic neuropathy by 9 weeks of age.

Microarray analyses on SCN isolated from 5- and 13-week mice were then performed to further characterize DN. Using a $FDR < 0.05$, we identified 1,184 and 1,941 DEGs associated with time in aging BTBR *ob/+* and *ob/ob* mice, respectively (Fig. 3A). Comparisons to determine changes associated with DN also identified 1,503 (624 up-regulated and 825 down-regulated) and 642 (331 up-regulated and 301 down-regulated) DEGs in the 5- and 13-week BTBR *ob/ob* mice compared to age-matched *ob/+* controls, respectively (Fig. 4A). The overlap among these DEG sets is summarized in Supplementary Table 3. RT-qPCR of select DEGs exhibiting the greatest fold-change reflected comparable profiles (Supplementary Fig. 2), validating the microarray findings.

To identify over-represented biological functions in the DEG sets, we performed GSEA and generated a heat map of the top biological terms and pathways (Fig. 4B). Comparison of 5 to 13 week data revealed changes related to aging which were relatively similar for both BTBR *ob/ob* and *ob/+* genotypes; however, BTBR *ob/ob* mice demonstrated enrichment in membrane trafficking and endocytosis-related terms. When BTBR *ob/+* were compared to *ob/ob* at 5 and 13 weeks to determine changes related to DN, the most significantly enriched hits were related to inflammation and the immune response. Notably, the level of regulation as well as the number of associated terms and pathways within these categories was increased at the earlier 5 week time point. We also observed significant enrichment of hits related to chemotaxis at 5 weeks, and MMP12 was the most significantly upregulated gene at both time points (Supplementary Fig. 2). Together, these data suggest that inflammatory mechanisms may play a critical role in early DN development and DN progression.

To complement these analyses and further identify common DEGs and differentially regulated pathways related to DN across diabetes mouse models, we compared our 5 and 13 week data sets to our previously published data set from 24 week C57BKS *db/db* mice (17), an established DN mouse model. Briefly, C57BKS *db/db* mice display decreased motor and sensory NCVs between 8–12 weeks and decreased IENF density at 18 weeks (10). Within these three data sets, we identified 189 common DEGs (Fig. 4A) which are listed along with their respective fold-changes in Supplementary Table 4. Interestingly, a number of cytokines and inflammatory mediators are represented across models and ages, and MMP12, the most highly dysregulated gene in BTBR *ob/ob* mice, is also significantly dysregulated in C57BKS *db/db* mice. GSEA analysis (Fig. 4B) demonstrated that all three data sets exhibited significant upregulation of immune response-related terms and functions; however, the BTBR *ob/ob* mice at each age exhibited a larger number of terms and pathways within this category compared to the C57BKS *db/db* mice, as well as increased levels of dysregulation. We also noted that terms and functions related to lipid metabolism were upregulated only in the C57BKS *db/db* mice, while those related to neuronal differentiation and outgrowth were downregulated. Overall, these comparisons again support a potential role for inflammation and the immune response in DN.

Finally, to further characterize inflammation within the nerve environment, we examined the levels of select cytokines and chemokines in SCN protein lysates. While no significant

differences between BTBR *ob/+* and *ob/ob* mice were observed at 5 weeks, at 13 weeks we saw significant increases in the levels of IL-10, CCL11, CXCL1, and CXCL10, as well as a trending increase in IL-6 in BTBR *ob/ob* SCN relative to levels in *ob/+* SCN (Fig. 5A–E). Similar to the gene expression data demonstrating a higher representation of inflammation and immune response-related terms at the earlier 5 week time point, we also observed decreases in CCL11 and CXCL1 protein levels at 13 weeks compared to at 5 weeks in BTBR *ob/ob* mice. Finally, MMP12 protein levels were consistently increased at each time point in BTBR *ob/ob* mice, as seen in the gene expression arrays (Fig. 5F).

DISCUSSION

As the T2D pandemic continues to escalate, there is a critical need for novel animal models that recapitulate the associated diabetic complications in order to develop effective treatment strategies. This is particularly important for DN, a debilitating and common complication with no effective treatments. The current studies demonstrate that BTBR *ob/ob* mice exhibit numerous features of DN, including thermal hypoalgesia, delayed NCVs, and reduced IENF density. Furthermore, our gene expression profiling analyses suggest that many inflammatory mediators within the peripheral nerve are dysregulated in diabetes, strengthening the emerging idea that inflammation may contribute to DN pathophysiology in T2D. Thus, we anticipate that BTBR *ob/ob* mice are a favorable model for disease pathogenesis and therapeutic development studies due to the rapid and robust disease onset and progression.

Despite the surge in diabetes-related studies, the repertoire of available mouse models where DN has been characterized remains limited (10,16). Furthermore, these models are on varying background strains, model both type 1 (T1D) and T2D, and analyses are reported with differing diabetes durations, at different ages, and with different genders; factors which can all impact phenotypes. Data indicate that *ob/ob* mice are susceptible to more robust diabetes on the BTBR background compared to the C57BL6 background (14), and we and others have shown that BTBR *ob/ob* mice are hyperphagic and exhibit early and robust diabetes along with evidence of dyslipidemia as early as 5 weeks of age (Fig. 1, Supplementary Fig. 1; (11,13,14)). BTBR *ob/ob* mice also exhibit a number of microvascular complications associated with diabetes, including nephropathy, cardiomyopathy, and fatty liver disease (13,24), suggesting that they may represent an ideal model for diabetic complications research; however, the impact of T2D on the peripheral nervous system in BTBR *ob/ob* mice was not known prior to the current study.

Our goal was to characterize neuropathy in BTBR *ob/ob* mice. We demonstrate that BTBR *ob/ob* mice exhibit increased thermal latency and decreased MNCV and SNCV by 9 weeks and reduced IENF density at 13 weeks (Fig. 2). Reports on established leptin-based models, including the C57BKS *db/db* and C57BL6 *ob/ob* mice, exhibit the presence of DN pathology beginning as early as 8 weeks and 11 weeks, respectively, while C57BL6 *db/db* mice only exhibit significant DN outcomes at 24 weeks when fed a high-fat diet (10). Interestingly, our BTBR *ob/ob* data demonstrate 29% and 40% decreases in MNCV at 9 and 13 weeks, respectively, whereas C57BL6 *ob/ob* mice exhibit a 22% decrease at 11 weeks (14), suggesting that BTBR *ob/ob* mice develop a more rapid and robust DN phenotype.

This is not unexpected given the increased diabetes severity in BTBR *ob/ob* mice relative to C57BL6 *ob/ob* mice (11,13,14).

While we acknowledge that leptin-based models have limitations and alternative mouse background- and leptin-dependent effects may impact phenotypes (11,12,14), our results support BTBR *ob/ob* mice as a valid model for DN research. Because these animals develop other microvascular complications (13,24), they also provide a means to study common mechanisms that underlie DN and other diabetic complications. In addition, the leptin deficiency in BTBR *ob/ob* mice offers an opportunity to examine the reversibility of diabetic complications using exogenous leptin treatment, an approach not possible in models based on leptin receptor mutations (25).

To examine potential mechanisms underlying DN pathogenesis, we performed gene expression profiling on SCN from 5- and 13-week BTBR *ob/ob* and *ob/+* mice (Fig. 3). Using our in-house bioinformatics pipeline (17), we found that aging BTBR *ob/ob* mice demonstrate dysregulation of pathways related to endocytosis and membrane trafficking between 5 and 13 weeks, and that some of the most highly regulated DEGs are related to the humoral response, suggesting that immune dysregulation within the nerve environment may contribute to DN progression. We observed a 5.02- and 6.33-fold increase in *Ighg1* and *Ighg2*, respectively, in BTBR *ob/ob* mice at 13 weeks, and previous studies demonstrate that IgGs are elevated in T2D patients and are strongly associated with diabetic nephropathy in T1D patients (26). Furthermore, increased IgG deposition is observed in the kidney of NOD mice, a T1D model, likely due to infiltrating B cells (27). Likewise, we observed significant overrepresentation of inflammation and immune response pathways in BTBR *ob/ob* mice at both 5 and 13 weeks. Interestingly, the level of differential expression and the number of DEGs within the inflammation and immune response categories were significantly increased at the earlier time point, which may suggest that these pathways may underlie DN onset. As we are unable to ascertain at this point whether inflammation plays a causal contribution to DN or if inflammation is a consequence of diabetes itself with no bearing on DN progression, further in-depth experimental analyses are necessary to explore the role of inflammation in the nerve environment.

Inflammation is gaining momentum as a potential driving mechanism in the development and progression of diabetic microvascular complications. Emerging evidence strongly supports a role for inflammation in the progression of diabetic retinopathy and nephropathy (28,29), and cross-sectional and prospective studies have demonstrated elevated levels of circulating inflammatory mediators, including cytokines, chemokines, and acute-phase proteins, in the blood of T2D patients (30,31). In a rat nerve injury model, infiltration of inflammatory cells and an increase of cytokines is observed in the SCN (32–34); however, little is known about the role of inflammation in DN in T1D and T2D models. In BTBR *ob/ob* mice, we observed significant elevation of IL-10, CCL11, CDCL1, and CXCL10 at 13 weeks, as well as an increasing trend for IL-6. In streptozotocin (STZ)-injected C57BL6 mice, a model of T1D, the pro-inflammatory molecules IL-6, TNF- α , and IL-1 β were elevated in SCN (35–37). In T2D patients, IL-6 is elevated in sural nerve perineurium (37), and increased NF- κ B activity, a transcription factor responsible for generating a number of immune-related mediators, is also observed in T2D patient sural nerves (38). Gene

expression profiling studies on T1D and T2D human subjects with progressive DN also implicate inflammation (21). Therefore, our recent observation of several inflammation pathways in BTBR *ob/ob* mice strengthens the emerging idea that inflammation plays a role in the pathophysiology of DN.

Of note, the SCN includes a heterogeneous mix of Schwann cells, nerves, fibroblasts, adipocytes, and vascular endothelial cells (39) as well as resident and infiltrating non-neuronal cells; therefore, it is possible that the observed alterations may be driven by cell types other than the nerves. In addition, it is also possible that circulating immune cells may be recruited into peripheral nerves during DN, similar to observations in diabetic retinopathy and nephropathy (40,41). Our data demonstrate that CCL2, a chemokine strongly associated with inflammatory cell recruitment to sites of injury (42), was among the significantly increased DEGs (fold change of 2.88 at 5 weeks). While we did not detect CCL2 in our SCN protein profiling analysis, elevated CCL2 levels are observed in peripheral blood of T2D patients (43), and increased CCL2 is present in C57BL6 *ob/ob* mouse plasma (44). Furthermore, our protein profiling data demonstrates that other classical mediators of chemotaxis, including CCL11, CXCL1, and CXCL10, are upregulated in BTBR *ob/ob* mouse SCN at 13 weeks (Fig. 5A–D), and chemotaxis terms and pathways are overrepresented at 5 weeks (Fig. 3, 4). Finally, MMP12 was the highest upregulated gene at both 5 and 13 weeks, and increased MMP12 protein was also present in BTBR *ob/ob* SCN (Supplementary Fig. 2, Fig. 5E). MMPs are involved in extracellular matrix breakdown during normal physiological processes and in disease conditions (45) and are expressed in activated macrophages (46) and Schwann cells (47), further indicating that chemotaxis and recruitment of immune cells may play a role in DN pathogenesis. Given that blocking chemotaxis using a CCR2 antagonist in C57BKS *db/db* mice or knocking out CCL2 in C57BL6 *db/db* mice attenuates diabetic nephropathy (40,48), further investigation into therapies targeting chemokines identified in BTBR *ob/ob* mice or those targeting MMP12 activity may be warranted for DN. In addition, future studies investigating the source of altered immune mediators, whether they are associated with infiltrating cells or produced by resident cells, are also warranted to gain additional insight into potential therapeutic targets in DN.

Also of interest are the results and implications stemming from our protein multiplex analyses. Though our protein array data do not exhibit significant differences at 5 weeks of age, this could be explained by the potential variability in the diabetic status of the BTBR *ob/ob* mice as this time point coincides with hyperglycemia onset. Thus, not all mice may exhibit a robust diabetic phenotype at 5 weeks. In support of this contention, we performed a Pearson correlation on our 5 week MMP12 protein data and found that MMP12 levels correlate with increased levels of %GHb (0.86; $P = 0.0003$). Additional longitudinal measurements of the selected cytokines between 4–13 weeks with increased sample sizes may provide less variable outcomes and a clearer picture of any associated alterations in the levels of these mediators throughout the DN disease course.

We also observed a decrease in inflammatory mediators between 5 and 13 weeks for both the diabetic and control mice, a finding that could be attributed to the ongoing nerve developmental processes at the early time point. Chemokines, including CCL5 (49) and

CXCL12 (50), are essential for the development and organization of the hematopoietic/lymphopoietic system and are expressed by different types of cells in the nervous system. Thus, the cytokines that were significantly increased in our 5 week array data may reflect these early processes. While the levels decrease once the nervous system is fully developed in the BTBR *ob/+* mice, these levels do not drop to same extent in the diabetic BTBR *ob/ob* mice. We speculate that hyperglycemia and the associated oxidative stress in the diabetic nerve environment could account for the observed persistence of these inflammatory mediators in BTBR *ob/ob* mice.

Though the gene expression data demonstrate increased dysregulation of immune related categories at the earlier 5 week time point, our protein data do not exhibit significant differences until 13 weeks. One explanation is that steady-state transcript levels can only partially predict protein levels due to the intricate, heavily regulated processes that span mRNA processing to the post-processed proteome (51). Of the cytokines measured using the multiplex assay CXCL1 (at 13 weeks) and MMP12 (at 5 and 13 weeks) are differentially expressed in our microarray data set. Measuring the protein products of other dysregulated immune-related genes identified in our GSEA (Supplementary Table 4) could likely provide a more complete reflection of the inflammation and immune response pathways that occur in the BTBR *ob/ob* mice at 5 weeks. The protein levels of some of these targets will be assessed in subsequent studies.

Comparison of 5- and 13-week BTBR *ob/ob* DEGs with 24-week C57BKS *db/db* mouse data identified 189 shared DEGs and a number of common biological functions (Fig. 4A; Supplementary Table 4). Again, MMP12 was significantly upregulated in C57BKS *db/db* mice, reflecting levels 6.6-fold higher than controls. In addition, changes consistent with demyelination were observed across the 3 datasets. Genes encoding the myelin structural proteins PMP22, MPZ, and ELOVL6 were down-regulated at 5 and 13 weeks and may represent early Schwann cell abnormalities that precede the structural changes of demyelination. Segmental demyelination has been observed in human DN (52), but evidence of structural abnormalities is lacking in mouse models, potentially because of the shorter disease course relative to humans. Interestingly, no chemokines were included among the 189 common DEGs, suggesting that these changes may be strain- and age-dependent; however, a number of other inflammation-related DEGs were common, including *Il1rn*, *Il7r*, and *Tlr13*. These are reflected in the overrepresented terms related to inflammation, the immune response, and chemotaxis which are shared among models following the functional enrichment analyses.

In summary, a single model that manifests every aspect of human DN does not exist; however, BTBR *ob/ob* mice exhibit robust DN and provides a great opportunity to elucidate the molecular mechanisms and investigate novel therapies for DN. Our data further suggest that inflammation may underlie DN development and progression, and future studies examining the role of inflammation and the immune response in DN are warranted.

Supplementary Material

Refer to Web version on PubMed Central for supplementary material.

Acknowledgments

The authors would like to thank Mrs. Judith Bentley for excellent administrative support during the preparation of this manuscript. We also acknowledge the technical expertise of Ms. Jacqueline Dauch, Ms. Chelsea Lindblad and Dr. Sang Su Oh in conducting animal experiments, Mrs. Yu Hong for RNA processing, and Dr. Diane Bender for immunology-related consultation. The authors thank the Hormone Core and Lipid Laboratory at the Mouse Metabolic Phenotyping Center at Vanderbilt University for mouse plasma insulin and lipid measurements, and the Chemistry Core of the MDRTC (930DK020572) at the U-M for mouse %GHb measurements. The authors thank the Segal Laboratory at the U-M for the use of equipment required to perform Milliplex immunoassays. The authors would also like to thank Dr. Charlie Alpers at the University of Washington for expert advice on the BTBR *ob/ob* mouse strain.

Funding was provided by the National Institutes of Health (1DP3DK094292, 1R24082841 to E.L.F.), the Juvenile Diabetes Research Foundation (Post-doctoral Fellowship to J.H.), the American Diabetes Association, the Program for Neurology Research & Discovery, and the A. Alfred Taubman Medical Research Institute.

References

1. International Diabetes Federation. IDF Diabetes Atlas. 6. Brussels, Belgium: International Diabetes Federation; 2013. <http://www.idf.org/diabetesatlas>
2. Centers for Disease Control and Prevention. National diabetes fact sheet: national estimates and general information on diabetes and prediabetes in the United States, 2011. Atlanta, GA: U.S. Department of Health and Human Services, Centers for Disease Control and Prevention; 2011.
3. Malik RA, Tesfaye S, Ziegler D. Medical strategies to reduce amputation in patients with type 2 diabetes. *Diabet Med*. 2013; 30:893–900. [PubMed: 23445087]
4. Vincent AM, Callaghan BC, Smith AL, Feldman EL. Diabetic neuropathy: cellular mechanisms as therapeutic targets. *Nat Rev Neurol*. 2011; 7:573–583. [PubMed: 21912405]
5. Fernyhough P, Roy Chowdhury SK, Schmidt RE. Mitochondrial stress and the pathogenesis of diabetic neuropathy. *Expert Rev Endocrinol Metab*. 2010; 5:39–49. [PubMed: 20729997]
6. Wiggan TD, Sullivan KA, Pop-Busui R, Amato A, Sima AA, Feldman EL. Elevated triglycerides correlate with progression of diabetic neuropathy. *Diabetes*. 2009; 58:1634–1640. [PubMed: 19411614]
7. Vincent AM, Hayes JM, McLean LL, Vivekanandan-Giri A, Pennathur S, Feldman EL. Dyslipidemia-induced neuropathy in mice: the role of oxLDL/LOX-1. *Diabetes*. 2009; 58:2376–2385. [PubMed: 19592619]
8. O'Brien PD, Hinder LM, Sakowski SA, Feldman EL. ER stress in diabetic peripheral neuropathy: A new therapeutic target. *Antioxidants & redox signaling*. 2014; 21:621–633. [PubMed: 24382087]
9. Wilson N, Wright D. Inflammatory Mediators in Diabetic Neuropathy. *J Diabetes Metab*. 2011:S5.
10. O'Brien PD, Sakowski SA, Feldman EL. Mouse models of diabetic neuropathy. *ILAR journal / National Research Council, Institute of Laboratory Animal Resources*. 2014; 54:259–272.
11. Clee SM, Nadler ST, Attie AD. Genetic and genomic studies of the BTBR *ob/ob* mouse model of type 2 diabetes. *Am J Ther*. 2005; 12:491–498. [PubMed: 16280642]
12. Coppari R, Bjorbaek C. Leptin revisited: its mechanism of action and potential for treating diabetes. *Nat Rev Drug Discov*. 2012; 11:692–708. [PubMed: 22935803]
13. Hudkins KL, Pichaiwong W, Wietecha T, Kowalewska J, Banas MC, Spencer MW, Muhlfeld A, Koelling M, Pippin JW, Shankland SJ, Askari B, Rabaglia ME, Keller MP, Attie AD, Alpers CE. BTBR *Ob/Ob* mutant mice model progressive diabetic nephropathy. *Journal of the American Society of Nephrology : JASN*. 2010; 21:1533–1542. [PubMed: 20634301]
14. Keller MP, Choi Y, Wang P, Davis DB, Rabaglia ME, Oler AT, Stapleton DS, Argmann C, Schueler KL, Edwards S, Steinberg HA, Chaibub Neto E, Kleinhanz R, Turner S, Hellerstein MK, Schadt EE, Yandell BS, Kendzierski C, Attie AD. A gene expression network model of type 2 diabetes links cell cycle regulation in islets with diabetes susceptibility. *Genome Res*. 2008; 18:706–716. [PubMed: 18347327]
15. Sullivan KA, Lentz SI, Roberts JL Jr, Feldman EL. Criteria for creating and assessing mouse models of diabetic neuropathy. *Curr Drug Targets*. 2008; 9:3–13. [PubMed: 18220709]

16. Sullivan KA, Hayes JM, Wiggin TD, Backus C, Su Oh S, Lentz SI, Brosius F 3rd, Feldman EL. Mouse models of diabetic neuropathy. *Neurobiol Dis.* 2007; 28:276–285. [PubMed: 17804249]
17. Pande M, Hur J, Hong Y, Backus C, Hayes JM, Oh SS, Kretzler M, Feldman EL. Transcriptional profiling of diabetic neuropathy in the BKS db/db mouse: a model of type 2 diabetes. *Diabetes.* 2011; 60:1981–1989. [PubMed: 21617178]
18. Dai M, Wang P, Boyd AD, Kostov G, Athey B, Jones EG, Bunney WE, Myers RM, Speed TP, Akil H, Watson SJ, Meng F. Evolving gene/transcript definitions significantly alter the interpretation of GeneChip data. *Nucleic Acids Res.* 2005; 33:e175. [PubMed: 16284200]
19. Gautier L, Cope L, Bolstad BM, Irizarry RA. affy--analysis of Affymetrix GeneChip data at the probe level. *Bioinformatics.* 2004; 20:307–315. [PubMed: 14960456]
20. Wang X, Spandidos A, Wang H, Seed B. PrimerBank: a PCR primer database for quantitative gene expression analysis, 2012 update. *Nucleic Acids Res.* 2012; 40:D1144–1149. [PubMed: 22086960]
21. Hur J, Sullivan KA, Pande M, Hong Y, Sima AA, Jagadish HV, Kretzler M, Feldman EL. The identification of gene expression profiles associated with progression of human diabetic neuropathy. *Brain.* 2011; 134:3222–3235. [PubMed: 21926103]
22. Huang da W, Sherman BT, Lempicki RA. Systematic and integrative analysis of large gene lists using DAVID bioinformatics resources. *Nat Protoc.* 2009; 4:44–57. [PubMed: 19131956]
23. Huang da W, Sherman BT, Lempicki RA. Bioinformatics enrichment tools: paths toward the comprehensive functional analysis of large gene lists. *Nucleic acids research.* 2009; 37:1–13. [PubMed: 19033363]
24. O'Brien K, Kim J, Wietecha T, Hudkins K, McDonald T, Minami E, Alpers C. A new murine model of diabetic cardiomyopathy: The female leptin-deficient, black and tan brachyuric mouse. *Circulation.* 2009; 120:S490.
25. Harris RB, Zhou J, Redmann SM Jr, Smagin GN, Smith SR, Rodgers E, Zachwieja JJ. A leptin dose-response study in obese (ob/ob) and lean (+/?) mice. *Endocrinology.* 1998; 139:8–19. [PubMed: 9421392]
26. Virella G, Carter RE, Saad A, Crosswell EG, Game BA, Lopes-Virella MF. Distribution of IgM and IgG antibodies to oxidized LDL in immune complexes isolated from patients with type 1 diabetes and its relationship with nephropathy. *Clin Immunol.* 2008; 127:394–400. [PubMed: 18533284]
27. Xiao X, Ma B, Dong B, Zhao P, Tai N, Chen L, Wong FS, Wen L. Cellular and humoral immune responses in the early stages of diabetic nephropathy in NOD mice. *J Autoimmun.* 2009; 32:85–93. [PubMed: 19200691]
28. Tang J, Kern TS. Inflammation in diabetic retinopathy. *Prog Retin Eye Res.* 2011; 30:343–358. [PubMed: 21635964]
29. Wada J, Makino H. Inflammation and the pathogenesis of diabetic nephropathy. *Clin Sci (Lond).* 2013; 124:139–152. [PubMed: 23075333]
30. Spranger J, Kroke A, Mohlig M, Hoffmann K, Bergmann MM, Ristow M, Boeing H, Pfeiffer AF. Inflammatory cytokines and the risk to develop type 2 diabetes: results of the prospective population-based European Prospective Investigation into Cancer and Nutrition (EPIC)-Potsdam Study. *Diabetes.* 2003; 52:812–817. [PubMed: 12606524]
31. Herder C, Brunner EJ, Rathmann W, Strassburger K, Tabak AG, Schloot NC, Witte DR. Elevated levels of the anti-inflammatory interleukin-1 receptor antagonist precede the onset of type 2 diabetes: the Whitehall II study. *Diabetes Care.* 2009; 32:421–423. [PubMed: 19073760]
32. Okamoto K, Martin DP, Schmelzer JD, Mitsui Y, Low PA. Pro- and anti-inflammatory cytokine gene expression in rat sciatic nerve chronic constriction injury model of neuropathic pain. *Exp Neurol.* 2001; 169:386–391. [PubMed: 11358451]
33. Schmid AB, Coppieters MW, Ruitenber MJ, McLachlan EM. Local and remote immune-mediated inflammation after mild peripheral nerve compression in rats. *J Neuropathol Exp Neurol.* 2013; 72:662–680. [PubMed: 23771220]
34. Camara CC, Ramos HF, da Silva AP, Araujo CV, Gomes AS, Vale ML, Barbosa AL, Ribeiro RA, Brito GA, Costa CM, Oria RB. Oral gabapentin treatment accentuates nerve and peripheral

inflammatory responses following experimental nerve constriction in Wistar rats. *Neurosci Lett*. 2013; 556:93–98. [PubMed: 24140003]

35. Valsecchi AE, Franchi S, Panerai AE, Rossi A, Sacerdote P, Colleoni M. The soy isoflavone genistein reverses oxidative and inflammatory state, neuropathic pain, neurotrophic and vasculature deficits in diabetes mouse model. *Eur J Pharmacol*. 2011; 650:694–702. [PubMed: 21050844]
36. Kellogg AP, Wiggin TD, Larkin DD, Hayes JM, Stevens MJ, Pop-Busui R. Protective effects of cyclooxygenase-2 gene inactivation against peripheral nerve dysfunction and intraepidermal nerve fiber loss in experimental diabetes. *Diabetes*. 2007; 56:2997–3005. [PubMed: 17720896]
37. Bierhaus A, Haslbeck KM, Humpert PM, Liliensiek B, Dehmer T, Morcos M, Sayed AA, Andrassy M, Schiekofer S, Schneider JG, Schulz JB, Heuss D, Neundorfer B, Dierl S, Huber J, Tritschler H, Schmidt AM, Schwaninger M, Haering HU, Schleicher E, Kasper M, Stern DM, Arnold B, Nawroth PP. Loss of pain perception in diabetes is dependent on a receptor of the immunoglobulin superfamily. *J Clin Invest*. 2004; 114:1741–1751. [PubMed: 15599399]
38. Bierhaus A, Schiekofer S, Schwaninger M, Andrassy M, Humpert PM, Chen J, Hong M, Luther T, Henle T, Kloting I, Morcos M, Hofmann M, Tritschler H, Weigle B, Kasper M, Smith M, Perry G, Schmidt AM, Stern DM, Haring HU, Schleicher E, Nawroth PP. Diabetes-associated sustained activation of the transcription factor nuclear factor-kappaB. *Diabetes*. 2001; 50:2792–2808. [PubMed: 11723063]
39. Verheijen MH, Chrast R, Burrola P, Lemke G. Local regulation of fat metabolism in peripheral nerves. *Genes & development*. 2003; 17:2450–2464. [PubMed: 14522948]
40. Chow FY, Nikolic-Paterson DJ, Ma FY, Ozols E, Rollins BJ, Tesch GH. Monocyte chemoattractant protein-1-induced tissue inflammation is critical for the development of renal injury but not type 2 diabetes in obese db/db mice. *Diabetologia*. 2007; 50:471–480. [PubMed: 17160673]
41. Omri S, Behar-Cohen F, de Kozak Y, Sennlaub F, Verissimo LM, Jonet L, Savoldelli M, Omri B, Crisanti P. Microglia/macrophages migrate through retinal epithelium barrier by a transcellular route in diabetic retinopathy: role of PKCzeta in the Goto Kakizaki rat model. *Am J Pathol*. 2011; 179:942–953. [PubMed: 21712024]
42. Haberstroh U, Pocock J, Gomez-Guerrero C, Helmchen U, Hamann A, Gutierrez-Ramos JC, Stahl RA, Thaïss F. Expression of the chemokines MCP-1/CCL2 and RANTES/CCL5 is differentially regulated by infiltrating inflammatory cells. *Kidney Int*. 2002; 62:1264–1276. [PubMed: 12234296]
43. Nomura S, Shouzu A, Omoto S, Nishikawa M, Fukuhara S. Significance of chemokines and activated platelets in patients with diabetes. *Clin Exp Immunol*. 2000; 121:437–443. [PubMed: 10971508]
44. Sartipy P, Loskutoff DJ. Monocyte chemoattractant protein 1 in obesity and insulin resistance. *Proc Natl Acad Sci U S A*. 2003; 100:7265–7270. [PubMed: 12756299]
45. Lagente V, Le Quement C, Boichot E. Macrophage metalloelastase (MMP-12) as a target for inflammatory respiratory diseases. *Expert Opin Ther Targets*. 2009; 13:287–295. [PubMed: 19236151]
46. Wu L, Fan J, Matsumoto S, Watanabe T. Induction and regulation of matrix metalloproteinase-12 by cytokines and CD40 signaling in monocyte/macrophages. *Biochem Biophys Res Commun*. 2000; 269:808–815. [PubMed: 10720497]
47. Hughes PM, Wells GM, Perry VH, Brown MC, Miller KM. Comparison of matrix metalloproteinase expression during Wallerian degeneration in the central and peripheral nervous systems. *Neuroscience*. 2002; 113:273–287. [PubMed: 12127085]
48. Kang YS, Lee MH, Song HK, Ko GJ, Kwon OS, Lim TK, Kim SH, Han SY, Han KH, Lee JE, Han JY, Kim HK, Cha DR. CCR2 antagonism improves insulin resistance, lipid metabolism, and diabetic nephropathy in type 2 diabetic mice. *Kidney Int*. 2010; 78:883–894. [PubMed: 20686445]
49. Bolin LM, Murray R, Lukacs NW, Strieter RM, Kunkel SL, Schall TJ, Bacon KB. Primary sensory neurons migrate in response to the chemokine RANTES. *Journal of neuroimmunology*. 1998; 81:49–57. [PubMed: 9521605]

50. Belmadani A, Tran PB, Ren D, Assimacopoulos S, Grove EA, Miller RJ. The chemokine stromal cell-derived factor-1 regulates the migration of sensory neuron progenitors. *The Journal of neuroscience : the official journal of the Society for Neuroscience*. 2005; 25:3995–4003. [PubMed: 15843601]
51. Vogel C, Marcotte EM. Insights into the regulation of protein abundance from proteomic and transcriptomic analyses. *Nature reviews Genetics*. 2012; 13:227–232.
52. Malik RA, Veves A, Walker D, Siddique I, Lye RH, Schady W, Boulton AJ. Sural nerve fibre pathology in diabetic patients with mild neuropathy: relationship to pain, quantitative sensory testing and peripheral nerve electrophysiology. *Acta Neuropathol*. 2001; 101:367–374. [PubMed: 11355308]

Highlights

- BTBR *ob/ob* mice are obese, diabetic, and develop robust peripheral neuropathy by 9 weeks of age.
- Inflammation/immune mediator gene expression is altered in sciatic nerve during neuropathy
- BKS *db/db* mice exhibit similar inflammatory/immune alterations to those in seen BTBR *ob/ob* mice.
- MMP12, IL-10, CCL11, CXCL1, and CXCL10 are altered in sciatic nerve during neuropathy.

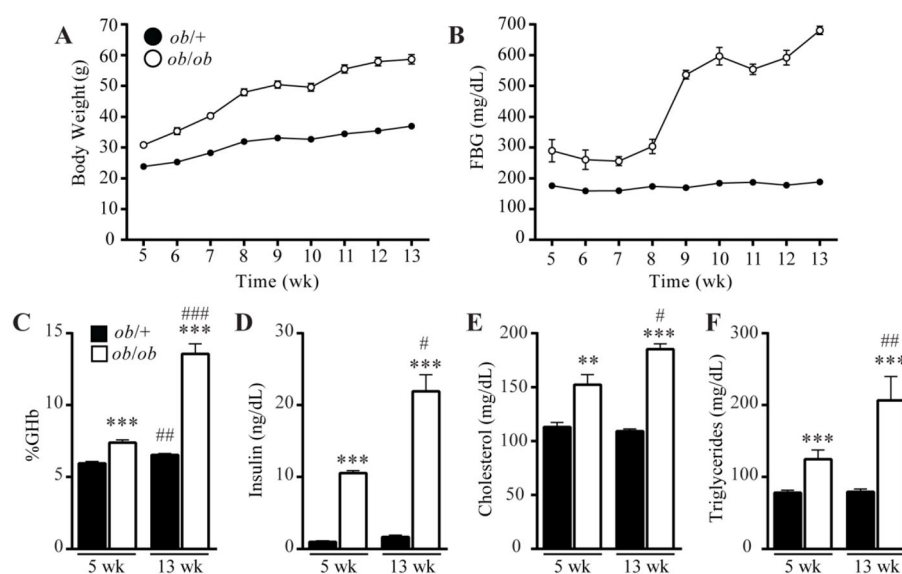


FIG. 1. Metabolic and lipid profile of BTBR *ob/ob* mice

A–B. BTBR *ob/+* (solid black circles) and *ob/ob* (open circles) mice were analyzed for body weight (A) and fasting blood glucose (B) at 5 weeks or weekly from 6 until 13 weeks of age. ANOVA confirms significance of the whole curves as well as between each data point. **C–F.** BTBR *ob/+* (solid bars) and *ob/ob* (open bars) mice underwent terminal glycosylated hemoglobin (%GHb; C), fasting plasma insulin (D), total plasma cholesterol (E), and total triglycerides (F) measurements at 5 and 13 weeks of age. Means \pm SEM, $n = 7$ –11 per group. *** $P < 0.0001$ vs. non-diabetic *ob/+* mice. # $P < 0.05$, ## $P < 0.001$; ### $P < 0.0001$ vs. 5 week mice.

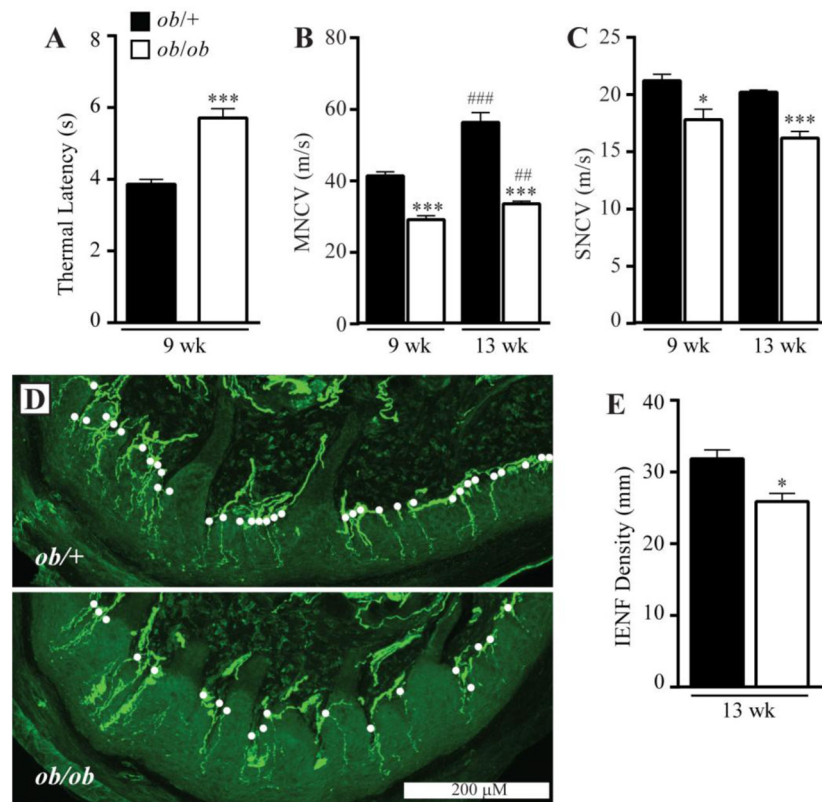


FIG. 2. BTBR *ob/ob* mice display robust neuropathy characterized by electrophysiological and morphological deficits

A. Response time of hindpaw withdrawal latency to thermal stimulus at 9 weeks of age. **B–C.** Analysis of sural (B; Motor NCV) and sciatic (C; Sensory NCV) nerve conduction velocity in BTBR *ob/+* (black bars) and *ob/ob* mice (open bars) at 9 and 13 weeks of age. **D.** Representative images of PGP 9.5-stained nerve fibers in BTBR *ob/+* (top) and *ob/ob* (bottom) mice density at 13 weeks of age. White circles indicate nerve fibers. Bar = 200 μ M. **E.** Quantification of IENF density in 13 week BTBR *ob/+* (black bar) and *ob/ob* (open bar) mice. Means \pm SEM, $n = 7-11$ per group. * $P < 0.05$; *** $P < 0.0001$ vs. non-diabetic *ob/+* mice. ## $P < 0.001$; ### $P < 0.0001$ vs. 9 week mice.

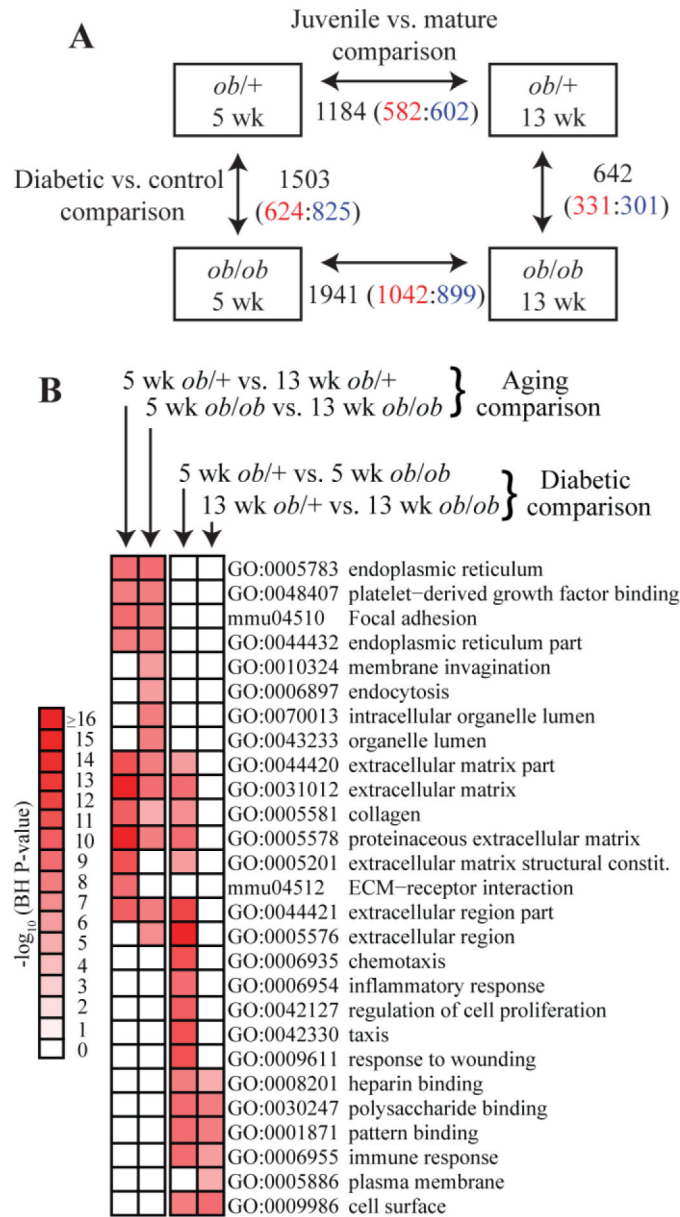


FIG. 3. Gene expression analyses in the SCN of BTBR *ob/ob* mice

RNA samples obtained from the SCN of BTBR *ob/+* and *ob/ob* mice at 5 and 13 weeks of age were hybridized to Affymetrix GeneChip microarrays. Data were analyzed to identify DEGs and functional enrichment analyses were performed to identify overrepresented biological categories and pathways. **A.** Data sets were compared using an IBMT FDR < 0.05 to identify DEGs. The number of DEGs from each comparison are indicated along each arrow; numbers in parentheses indicate the number of up- (red) and down- (blue) regulated DEGs in each dataset. **B.** Functional enrichment analysis using DAVID on the four DEG sets, including 5wk *ob/+*, 5wk *ob/ob*, 13wk *ob/+* and 13wk *ob/ob*. Benjamini-Horchberg (BH)-corrected P-values of the top 10 most significant functional terms are represented by heat-map with a log₁₀-based color and number index.

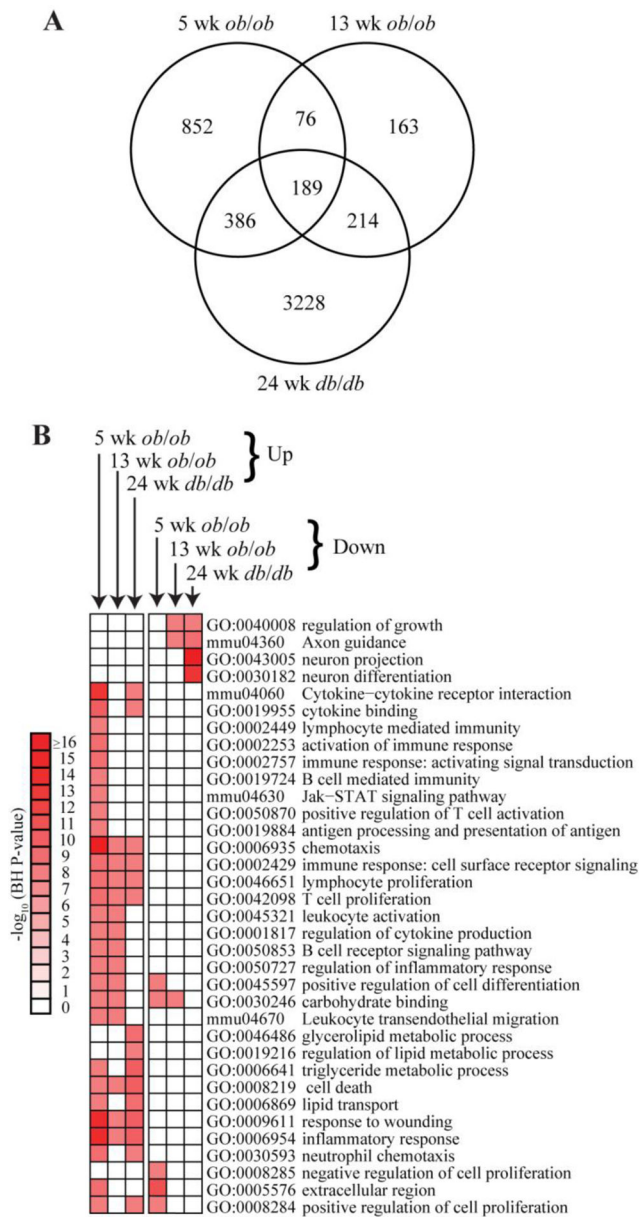


FIG. 4. Comparison of DEGs identified in BTBR *ob/ob* mice to those identified in another T2D DN model, the C57BKS *db/db* mouse

DEGs from 5 and 13 week BTBR *ob/ob* mice were compared to previously published DEGs from 24 week C57BKS *db/db* mice. A. Venn diagram demonstrating the number of common DEGs among the 3 datasets. B. Heat map demonstrating the top most significant up- and down-regulated functional categories in each dataset, represented using a \log_{10} -BH-corrected P value-based color and number index.

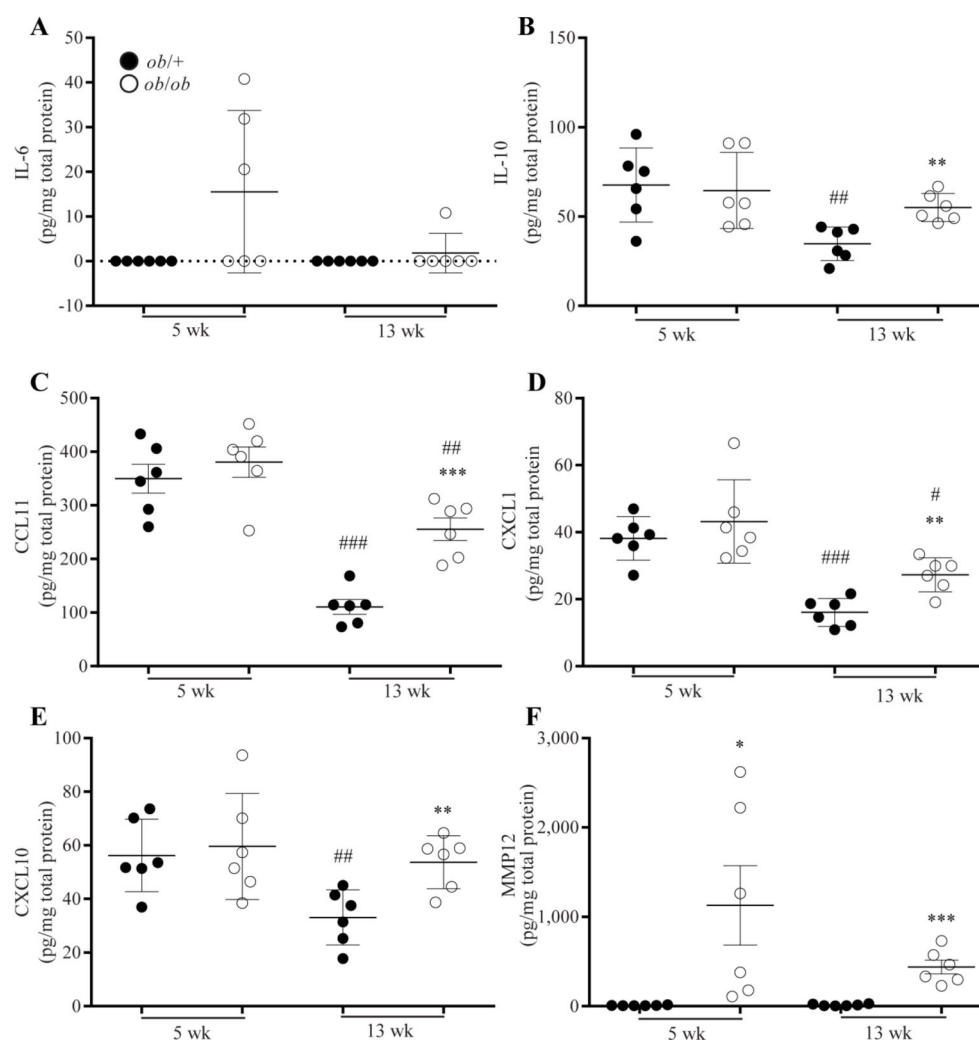


FIG 5. Cytokine and MMP protein levels in SCN of BTBR *ob/ob* mice

Protein levels of IL-6 (A), IL-10 (B), CCL11 (C), CXCL1 (D), CXCL10 (E) and MMP12 (F) in SCN of BTBR *ob/+* (black circles) and *ob/ob* (open circles) mice, measured using MILLIPLEX xMAP magnetic bead technology. * $P < 0.05$, ** $P < 0.01$, *** $P < 0.001$ vs. non-diabetic *ob/+* mice. # $P < 0.05$, ## $P < 0.01$, ### $P < 0.001$ vs. 5 week mice.